# Separation and Characterization of Vanadyl Porphyrins in Venezuela Orinoco Heavy Crude Oil

**ARTICLE** *in* ENERGY & FUELS · JUNE 2013

Impact Factor: 2.79 · DOI: 10.1021/ef400161p

energy&fuels

Article

pubs.acs.org/EF

# Separation and Characterization of Vanadyl Porphyrins in Venezuela Orinoco Heavy Crude Oil

Xu Zhao,[†] Yu Liu,[†] Chunming Xu,*[,†] Yuanyuan Yan,[†] Yahe Zhang,[†] Qingyu Zhang,[†] Suoqi Zhao,[†] Keng Chung,[‡] Murray R. Gray,[§] and Quan Shi*[,†]

[†]State Key Laboratory of Heavy Oil Processing, China University of Petroleum, Beijing 102249, People's Republic of China

[‡]Well Resources Incorporated, 3919-149A Street, Edmonton, Alberta T6R 1J8, Canada

[§]Department of Chemical and Materials Engineering, University of Alberta, Edmonton, Alberta T6G 2V4, Canada

Supporting Information

**ABSTRACT:** Venezuela Orinoco heavy crude oil was sequentially separated into several subfractions to determine the contents and types of vanadyl porphyrins contained in the products. Vanadium contents in each subfraction were detected using an atomic absorption spectrometer (AAS) combined with the characterization of vanadyl porphyrins by ultraviolet−visible (UV−vis) spectroscopy and positive-ion electrospray ionization (ESI) Fourier transform-ion cyclotron resonance mass spectrometry (FT-ICR MS). Six types of petroleum vanadyl porphyrins, which have been identified previously, were well-characterized with the detailed fractionation. Three new series of vanadyl porphyrins corresponding to molecules of $C_nH_mN_4VO_2$, $C_nH_mN_4VO_3$, and $C_nH_mN_4VO_4$, respectively, were identified in addition to the six known types of vanadyl porphyrins.

## 1. INTRODUCTION

Oxovanadium(IV) and nickel(II) complexes of alkyl porphyrins are widely distributed in petroleum, oil shales, and maturing sedimentary bitumen.[1] Since their discovery in crude oils and shales by Treibs,[2,3] who postulated that porphyrins formed from chlorophylls and hemes in the organisms, these compounds have been extensively studied. Petroporphyrin is of particular significance in research into the formation of petroleum. Several types of alkyl porphyrins have been discovered, with most of them containing the main structure of $N_4VO$. Among them, etio porphyrins (ETIO) and deoxophylloerythroetio porphyrins (DPEP) are the two most common vanadyl porphyrins found in petroleum. These compounds have a double-bond equivalence (DBE) of 17 and 18, respectively.[4] The DBE is defined as the number of double bonds plus rings. Other types of vanadyl porphyrins, such as dicyclic-deoxophylloerythroetio porphyrins (di-DPEP), rhodo-etio porphyrins (rhodo-ETIO), rhodo-deoxophylloerythroetio porphyrins (rhodo-DPEP), and rhodo-dicyclic-deoxophylloerythroetio (rhodo-di-DPEP) have also been identified in petroleum by ultraviolet−visible (UV−vis) spectroscopy and mass spectrometry (MS).[4−6]

The UV−vis spectroscopy is a commonly used analytical technique for identification and quantification of petroporphyrins, because of its high intensity and sensitivity of metalloporphyrins and metal-free porphyrins to electronic absorption of UV−vis radiation. However, because of the complex nature of the hydrocarbon mixture, it is difficult to characterize vanadyl porphyrins present in low concentrations. Therefore, sample pretreatment is needed to isolate and concentrate the petroporphyrins prior to characterization. The isolation of petroporphyrins from the bulk sample also reduces or eliminates interferences from other petroleum compounds during the analysis.

A number of methods have been attempted to isolate the metalloporphyrin compounds, including solubility class separation,[7] Soxhlet extraction,[8,9] vacuum sublimation,[7] and chromatographic techniques, such as high-performance liquid chromatography (HPLC)[10−14] and thin-layer chromatography.[8,9] During the process of isolation, porphyrins and non-porphyrins are separated from each other. Therefore, it should be possible to examine the compounds without interference from each other. However, the nature of non-porphyrins is still a matter of controversy. Fish et al.[15] investigated vanadyl porphyrin and non-porphyrin by comparison of their molecular sizes and polarities. However, as yet, no mass spectrometric evidence of non-porphyrins has been found.

In recent years, Fourier transform ion cyclotron resonance mass spectrometry (FT-ICR MS) has been used to quantify the composition of highly complex hydrocarbon mixtures. FT-ICR MS has the highest available broadband mass resolution, mass resolving power, and mass accuracy, which enables the assignment of a unique elemental composition to each peak in the mass spectrum.[16−21] Rodgers et al.,[22] Qian et al.,[23] and McKenna et al.[4] identified vanadyl porphyrins by positive-ion electrospray ionization (ESI) and atmospheric pressure photoionization (APPI) FT-ICR MS. Qian et al.[23,24] identified sulfur-containing porphyrins and nickel porphyrins by APPI FT-ICR MS. In addition, these studies revealed the underlying causes of why nickel porphyrins had not been identified in earlier analyses and highlight the need for sample enrichment even for ultrahigh-resolution mass spectrometry.

In this paper, vanadium compounds in methanol- and toluene-extracted fractions of Venezuela Orinoco heavy crude

**Received:** August 15, 2012
**Revised:** April 25, 2013
**Published:** May 23, 2013

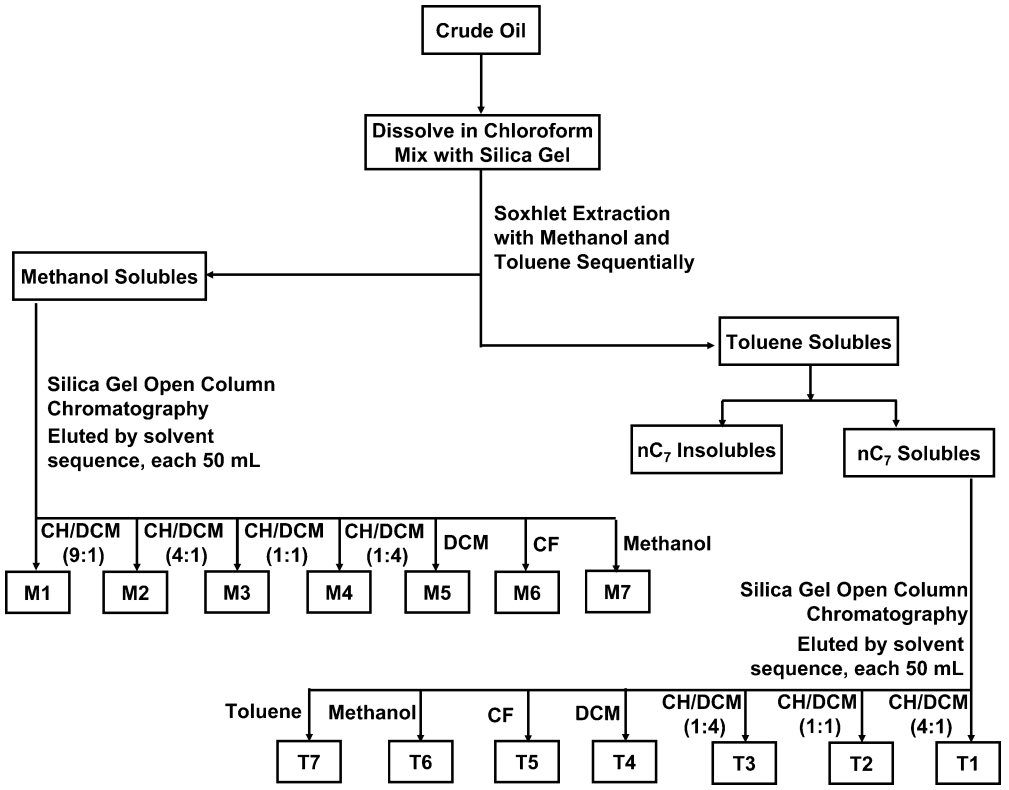


**Figure 1.** Separation scheme of vanadyl porphyrins in Venezuela Orinoco crude oil (CH, cyclohexane; DCM, dichloromethane; and CF, chloroform).

oil were characterized by positive-ion ESI FT-ICR MS and UV−vis spectroscopy.

## 2. EXPERIMENTAL SECTION

**2.1. Sample Pretreatment.** The Venezuela Orinoco heavy crude oil sample was obtained from the PetroChina refinery. The amount of elemental sulfur and nitrogen in the crude oil was 3.90 and 0.74 wt %, respectively. The density was 1.03 g/cm$^3$ at 20 °C. Nickel and vanadium concentrations were 68.93 and 513.31 wppm, respectively.

The crude oil sample was subjected to solvent extraction and silica gel chromatographic separation as shown in Figure 1. This sample fractionation scheme was modified from that used by Xu et al.[8,9] A total of 5 g of crude oil sample was dissolved in 60 mL of chloroform, followed by the addition of 40 g of silica gel to form a slurry mixture. The chloroform in the slurry mixture was evaporated at room temperature in a fume hood. The remaining oil/silica gel mixture was transferred into the thimble of the Soxhlet extractor using 300 mL of methanol and 300 mL of toluene sequentially as solvents. The Soxhlet extractions were performed for 40 and 24 h, respectively, yielding the methanol- and toluene-soluble fractions.

The methanol-soluble fraction was separated into various subfractions by introduction into a glass column (1 × 80 cm) packed with 100−200-mesh silica gel (about 50 cm high) and sequentially eluting with solvents (each 50 mL) of increasing polarity to yield various subfractions.

The toluene-soluble fraction was mixed with 50 mL of *n*-heptane ($n$C$_7$), and the mixture was refluxed for 30 min and then stored in the dark for 1 h. The $n$C$_7$ insolubles were obtained by filtration using 1−3 μm filter paper (ShuangQuan No. 202 filter paper) and rinsed with $n$C$_7$ for 0.5 h. The $n$C$_7$ insolubles on the filter paper were washed with 100 mL of toluene for 2 h and were obtained by evaporating the toluene from the filtrate. The $n$C$_7$ solubles were obtained by vacuum rotary evaporation of the filtrate from this extraction. The $n$C$_7$ solubles were fractionated into various subfractions in a glass column (1 × 80 cm) packed with 100−200-mesh silica gel (about 50 cm high) and sequentially eluting with solvents (each 50 mL) of increasing polarity to yield the various subfractions.

The vanadium content of each subfraction was determined using a graphite furnace atomic absorption spectrometer[25] (AAS, Beijing Puxi General Analytical Instrument Co., Ltd., TAS990). The samples were ashed in a muffle furnace at 550 °C for 12 h after ignition. The ash was dissolved in 2 mL of nitric acid and 0.5 mL of hydrochloric acid and then transferred to a 25 mL volumetric flask, where it was evenly mixed for measurement. A total of 10 μL of sample from the volumetric flask was introduced into the spectrometer to determine the vanadium content.

**2.2. UV−vis Spectroscopy Analysis.** UV−vis spectroscopy (UV-2102PCS spectrophotometer from Shanghai UNICO Instruments Co., Ltd.) was used to identify the metal porphyrins from the subfractions. The instrument was equipped with a 1 cm cuvette, and HPLC-grade toluene was used as the solvent. The samples were scanned at 300−700 nm wavelength.

**2.3. ESI FT-ICR MS Analysis.** A total of 10 mg of the crude oil sample and its subfractions were diluted with 1 mL of toluene. A total of 2−15 μL of each diluted sample was further diluted with 1 mL of toluene/methanol (1:1, v/v) solution to yield 0.02−0.15 mg/mL solution concentrations (resolved by the vanadium/porphyrin content). At this solution concentration range, the effect of molecular aggregation was minimized. A total of 5 μL of formic acid was added to the diluted test sample prior to the positive-ion ESI FT-ICR MS analysis using a Bruker apex-ultra FT-ICR MS equipped with a 9.4 T actively shielded superconducting magnet.

The test sample was infused through an Apollo II electrospray source at 180 μL/h using a syringe pump. The operating conditions for positive-ion formation were −4.0 kV emitter voltage, −4.5 kV capillary column front end voltage, and 320 V capillary column end voltage. Ions accumulated for 0.1 s in a hexapole with 2.4 V direct current (DC) voltage and 500 $V_{p-p}$ radio-frequency (RF) amplitude. The quadrupole (Q1) was optimized to obtain a broad range for ion transfers. An argon-filled hexapole collision cell was operated at 5 MHz and 700 $V_{p-p}$ RF amplitude, and ions accumulated for 0.6 s. The


dx.doi.org/10.1021/ef400161p | Energy Fuels 2013, 27, 2874−2882

extraction period for ions from the hexapole to the ion cyclotron resonance cell was set to 1.5 ms. The RF excitation was attenuated at 11.75 dB and used to excite ions from 200 to 1000 Da. Data sets (4 M) were acquired, and 128 scans were co-added to enhance the signal-to-noise ratio and dynamic range.

**2.4. ESI FT-ICR MS Data Processing.** FT-ICR MS was internally calibrated using a $N_1$ class homologous series $[C_nH_{2n-17}N_1 + H]^+$ and $[C_nH_{2n-19}N_1 + H]^+$. Internal quadratic calibration was also performed. Peaks with a relative abundance greater than 6 times the standard deviation of the baseline noise level were exported to a spreadsheet. Data analysis was performed by selecting a two-mass scale-expanded segment in the middle of the mass spectrum, followed by the detailed identification of each peak. The peak of at least one of each heteroatom class species was arbitrarily selected as a reference. Species with the same heteroatom class and their homologues with different DBE values and carbon numbers were searched within a set of 0.002 Kendrick mass defect tolerance. The details of the data analysis procedure used have been described elsewhere.[26]

## 3. RESULTS AND DISCUSSION

**3.1. Distribution of Vanadium in the Subfractions.** Table 1 shows the concentrations of vanadium in the methanol-soluble fraction, toluene-soluble fraction, and the subfractions obtained by silica gel chromatography. The amount of vanadium in the methanol- and toluene-soluble fractions was 58% and 39%, respectively, of the total vanadium in the feedstock. The majority of the vanadium compounds was enriched in M4, M5, and M6 of methanol-soluble subfractions, T3, T4, and T5 of $nC_7$-soluble subfractions, and the $nC_7$-insoluble fraction. The total yield in weight of all of the subfractions amounted to 94.17 wt %, representing about 93.21% of the total vanadium in the crude oil. Some of the vanadium may have been lost because of the absorption of a small amount of oil fractions onto the silica gel. This was evident from the coloration of the column following extraction.

**Table 1. Yield and Concentration of Vanadium in Subfractions**

| subfractions | yield[a] (wt %) | concentration of vanadium (wppm) | percentage of yield (%) |
|---|---|---|---|
| total methanol extract | 52.93 | 566.16 | 58.38 |
| total toluene extract | 42.26 | 469.14 | 38.62 |
| M1 | 38.23 | 22.42 | 1.67 |
| M2 | 0.92 | 113.26 | 0.20 |
| M3 | 1.78 | 130.83 | 0.45 |
| M4 | 6.99 | 2116.85 | 28.83 |
| M5 | 2.14 | 3113.62 | 12.98 |
| M6 | 1.55 | 4380.21 | 13.23 |
| M7 | 0.93 | 376.68 | 0.68 |
| T1 | 22.06 | 36.25 | 1.56 |
| T2 | 1.57 | 105.41 | 0.32 |
| T3 | 4.04 | 1453.04 | 11.44 |
| T4 | 2.14 | 1241.36 | 5.18 |
| T5 | 1.06 | 1477.53 | 3.05 |
| T6 | 1.33 | 571.49 | 1.48 |
| T7 | 5.02 | 94.11 | 0.92 |
| $nC_7$ insolubles | 4.41 | 1305.71 | 11.22 |

[a]On the basis of the crude oil.

**3.2. UV−vis Spectroscopy Analysis.** Panels a and b of Figure 2 show the UV−vis spectra of silica gel chromatographic M1−M3 subfractions and M4−M7 subfractions, respectively.

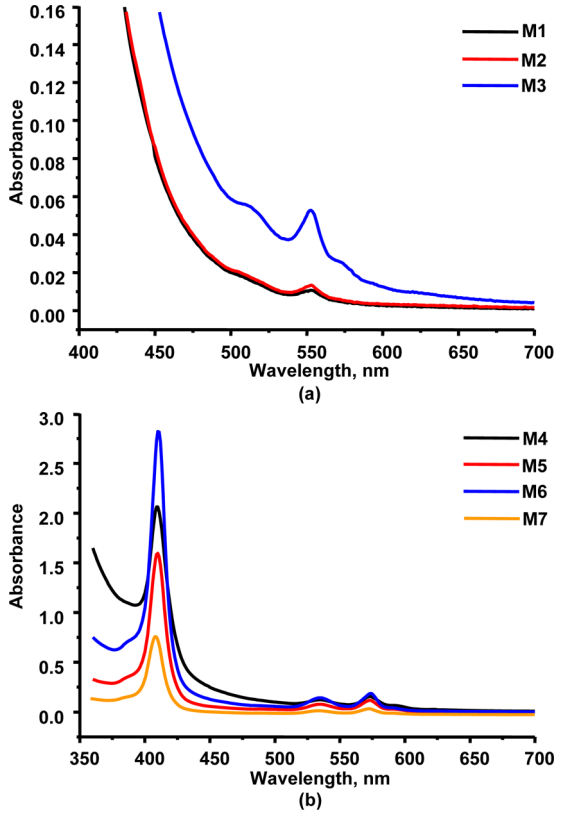


**Figure 2.** UV−vis spectra of silica gel chromatography subfractions of methanol extraction: (a) UV−vis spectra of M1−M3 and (b) UV−vis spectra of M4−M7.

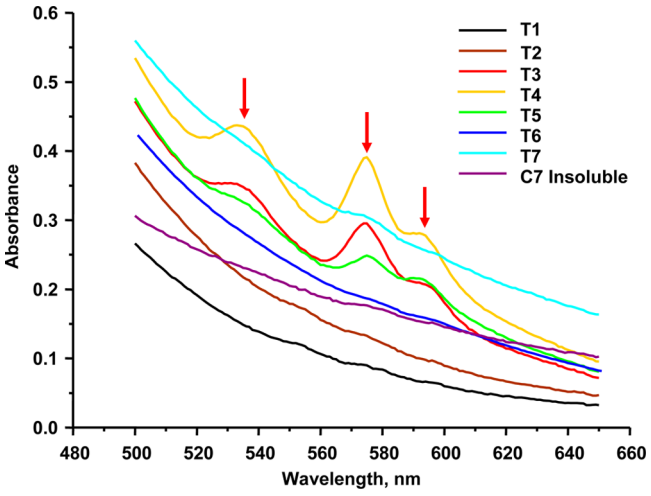


**Figure 3.** UV−vis spectra of silica gel chromatography subfractions of toluene extraction.

The characteristic UV−vis absorption band for nickel porphyrins was at the $\alpha$ band of 550 nm, whereas those for vanadyl porphyrins were at the Soret band of 410 nm, $\beta$ bands of 533 nm, and $\alpha$ band of 572 nm. The data presented in Table 1 and Figure 2 indicate that there is no correlation between vanadium contents of the (vanadium-rich) methanol subfractions (M4−M7) and their vanadium porphyrin contents.

Figure 3 shows the UV−vis spectra of silica gel chromatographic subfractions T1−T7 and $nC_7$ insolubles from the toluene extraction. No characteristic UV−vis absorption bands were observed for the T1, T2, T6, and T7 subfractions and $nC_7$


dx.doi.org/10.1021/ef400161p | Energy Fuels 2013, 27, 2874−2882

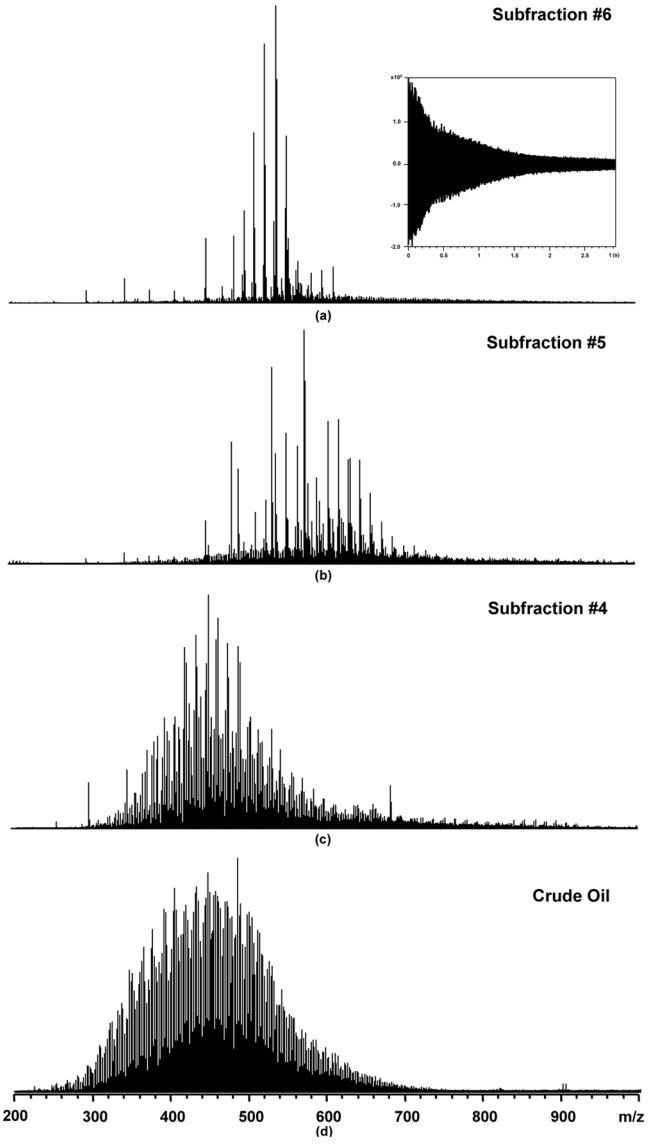


**Figure 4.** ESI FT-ICR MS broadband spectra at $m/z$ 200−1000: (a) Venezuela Orinoco crude oil and (b−d) subfractions M4, M5, and M6 of methanol extraction.

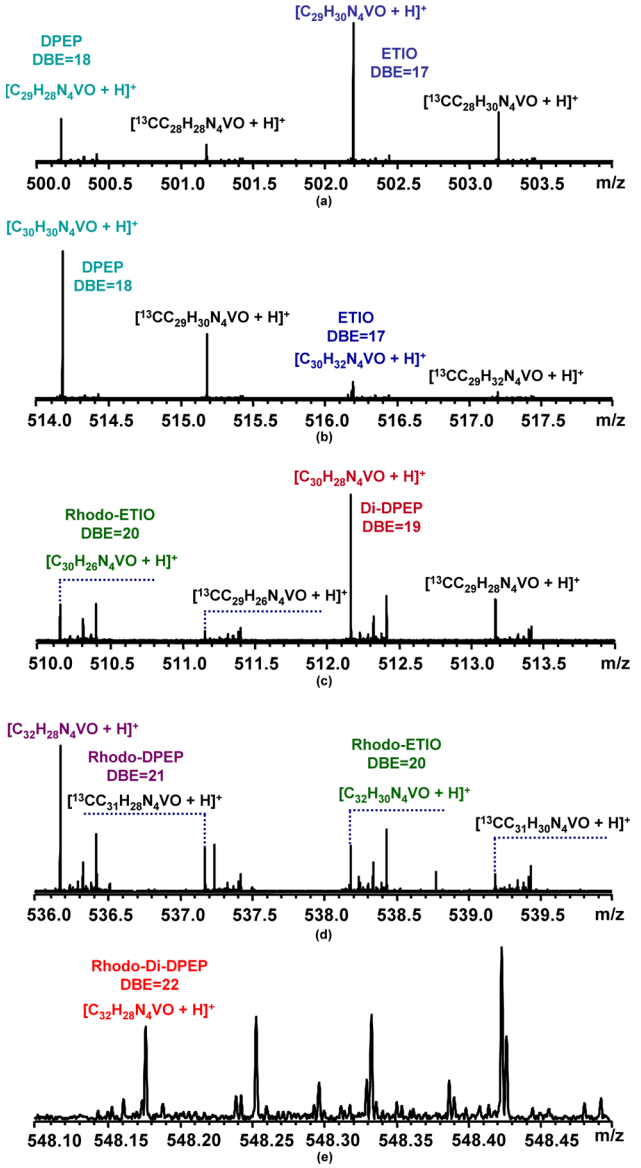


**Figure 5.** Expanded mass scale spectra for six types of vanadyl porphyrins in subfraction M6 of methanol extraction from the positive-ion ESI FT-ICR MS analysis: (a−e) at $m/z$ 500−504, 514−518, 510−514, 536−540, and 548, respectively.

insolubles, even though the concentration of vanadium in $nC_7$ insolubles was 1300 wppm. However, characteristic UV−vis absorption bands from vanadyl porphyrins were observed for T3, T4, and T5 subfractions. In addition, a shoulder peak at 590 nm for T3, T4, and T5 subfractions was observed. Freeman et al.[27] observed the peak locations for various vanadyl porphyrins in dichloromethane solvent using third derivative UV−vis spectroscopy and assigned the $\alpha$ bands of ETIO, DPEP, and benzo (rhodo) at 570.7, 573.0, and 578.7 nm, respectively. Factors such as the solvent used, peripheral substitution, coordination, and association could affect the location of the electronic absorption peaks, because they affect the electronic structure of the porphyrin macrocycle.[1] Although a red shift may occur, very little has been published on the absorption peak at 590 nm for vanadyl porphyrin.

**3.3. Characterization of Vanadyl Porphyrins in Methanol-Extracted Fractions by Positive-Ion ESI FT-ICR MS.** Figure 4 shows the positive-ion ESI FT-ICR MS broadband spectra of the crude oil sample and its M4, M5, and M6 subfractions. The mass distribution was distinct from each other. The abundant mass peaks in the M6 subfraction were vanadyl porphyrins. Figure 5 shows an expanded view of the segmental spectra of M6 at $m/z$ 500−504, 514−518, 510−514, 536−540, and 548. All six types of identified petroleum vanadyl porphyrins were found in M6, namely, ETIO, DPEP, rhodo-ETIO, rhodo-DPEP, di-DPEP, and rhodo-di-DPEP. However, only ETIO and DPEP was detected in the crude oil prior to separation (see Figure S1 of the Supporting Information). Hence, sample enrichment is a significant step in the identification and detection of the compounds, even when ultrahigh-resolution mass spectrometry is used. Figure 6 shows the distributions of these six types of vanadyl porphyrins in the M4, M5, and M6 subfractions. The DPEP ($C_nH_{2n-30}N_4V_1O_1$, corresponding to DBE = 18) was the most abundant vanadyl porphyrin detected in these subfractions. It has been proposed that the relative amounts of DPEP to ETIO porphyrins can be used to estimate the maturity of petroleum; young oils have high ratios of total DPEP to total ETIO ($\sum$DPEP/$\sum$ETIO).[28]


dx.doi.org/10.1021/ef400161p | Energy Fuels 2013, 27, 2874−2882

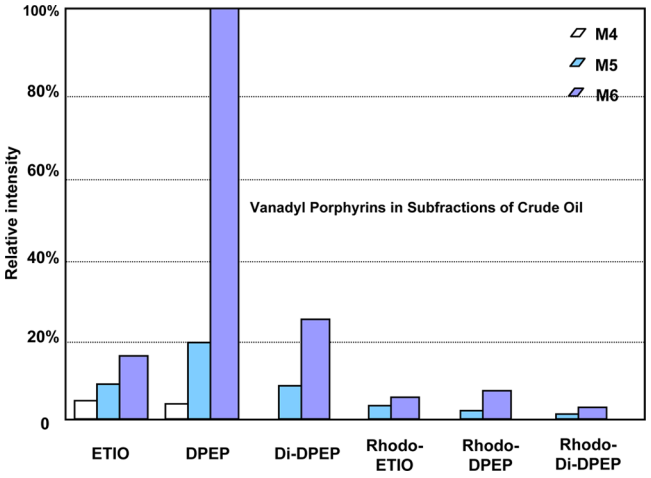


**Figure 6.** Distribution of various types of vanadyl porphyrins in subfractions M4−M6.

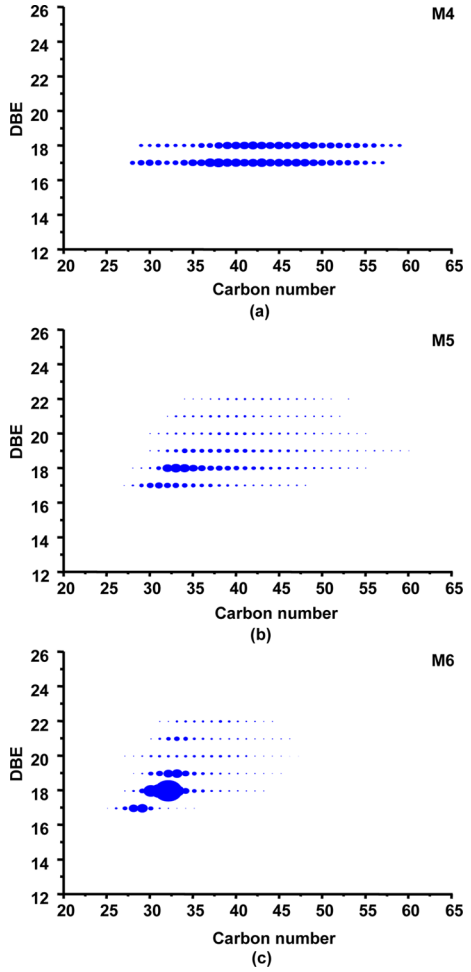


**Figure 7.** Iso-abundant plots of DBE as a function of the carbon number for each type of vanadyl porphyrins derived from positive-ion ESI FT-ICR MS: (a−c) subfractions M4−M6, respectively.

Figure 7 shows the iso-abundance plots of DBE as a function of the carbon number for vanadyl porphyrins in the M4, M5, and M6 subfractions, derived from positive-ion ESI FT-ICR mass spectra. Most ETIO ($C_nH_{2n-28}N_4V_1O_1$, corresponding to DBE = 17) and DPEP with long side chains were eluted to M4 during the silica gel chromatography. This is likely due to a relatively lower molecular polarity of ETIO and DPEP than other porphyrins. The carbon numbers of ETIO and DPEP were $C_{28}$−$C_{57}$ and $C_{29}$−$C_{59}$, respectively. The vanadyl porphyrins in M6 had shorter side chains with higher polarity compared to those in M5. The DPEPs with $C_{27}$−$C_{43}$ were the predominant type of porphyrins in M6, with a center of mass at $C_{32}$. The ETIOs had $C_{25}$−$C_{35}$, with a center of mass at $C_{29}$. The di-DPEPs had $C_{28}$−$C_{46}$, with a center of mass at $C_{33}$. The rhodo-ETIOs, rhodo-DPEPs, and rhodo-di-DPEPs had $C_{27}$−$C_{47}$, $C_{30}$−$C_{46}$, and $C_{31}$−$C_{44}$, respectively.

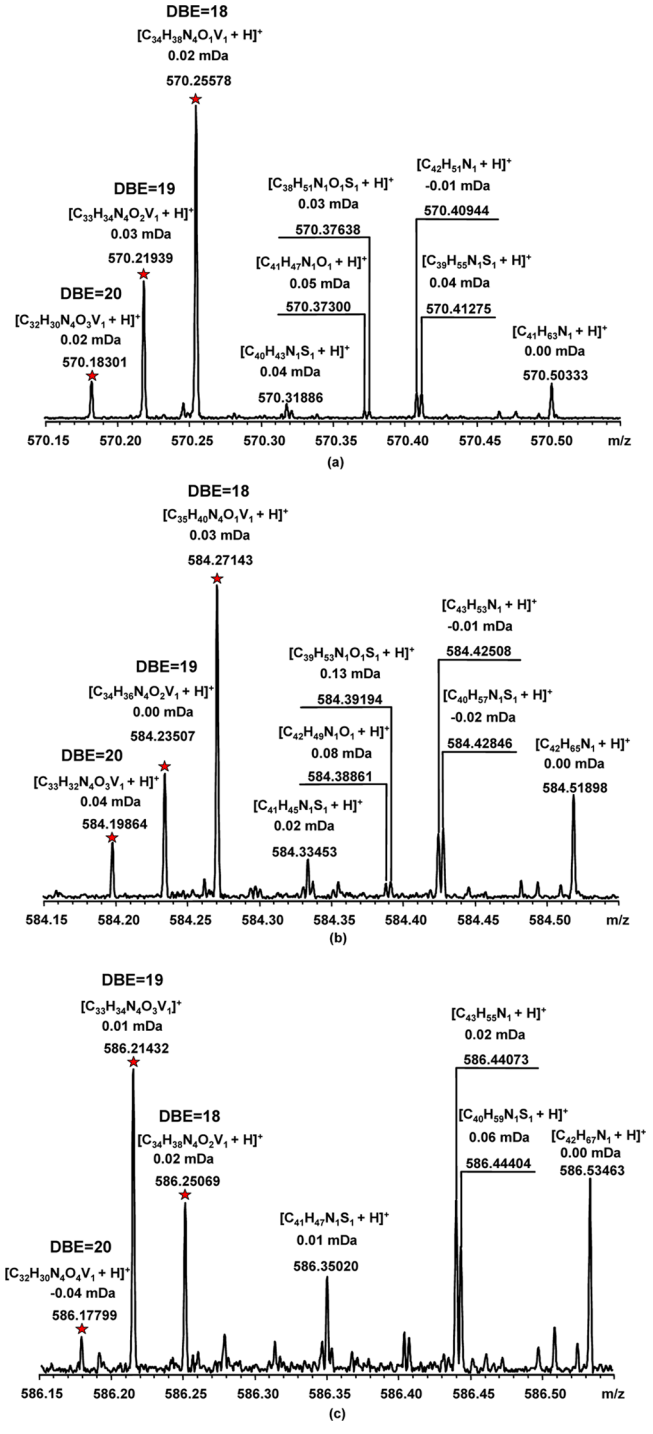


**Figure 8.** Expanded mass scale spectra of subfraction M6 from the positive-ion ESI FT-ICR MS analysis: (a−c) at *m*/*z* 570, 584, and 586, respectively.


dx.doi.org/10.1021/ef400161p | *Energy Fuels* 2013, 27, 2874−2882

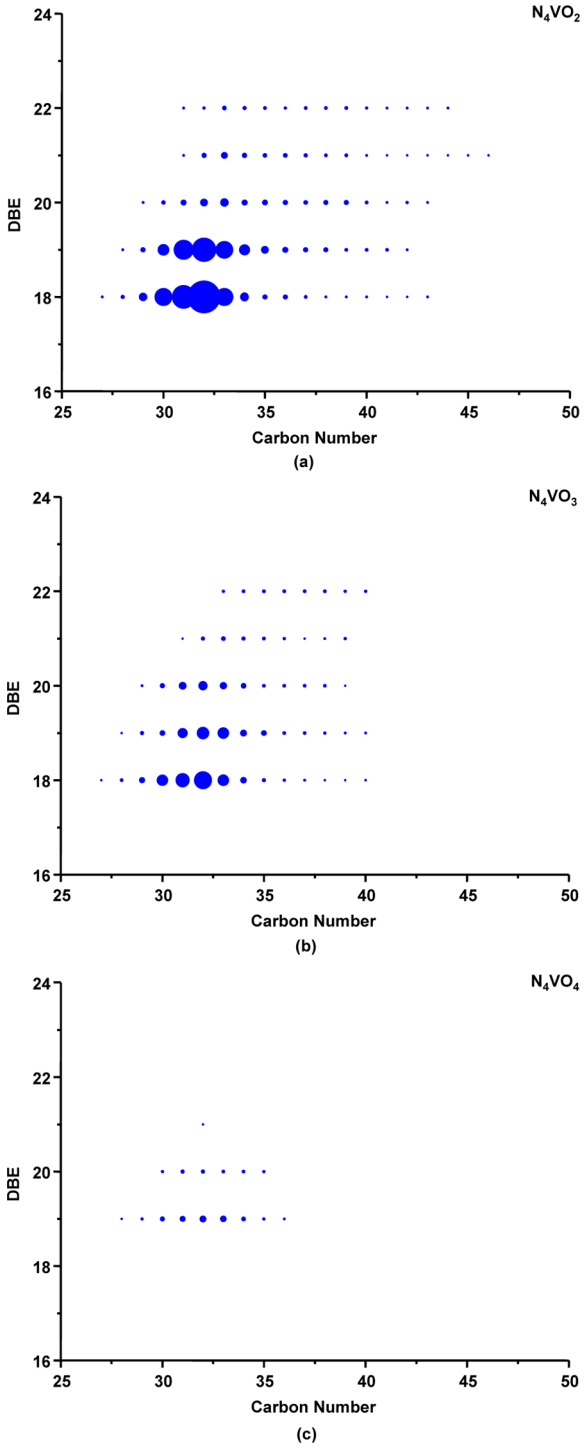


**Figure 9.** Iso-abundant plots of DBE as a function of the carbon number: (a–c) for $N_4V_1O_2$, $N_4V_1O_3$, and $N_4V_1O_4$ in subfraction M6 derived from positive-ion ESI FT-ICR MS, respectively.

**3.4. New Vanadyl Porphyrins Found in Methanol-Extracted Fractions.** The basic structure of porphyrin consists of four pyrrole units linked with four methine bridges, forming a cyclic planar molecule. The eight $\beta$-hydrogen atoms and the four hydrogen atoms on the methine bridges of porphyrin can be substituted, resulting in numerous possible structures for porphyrin compounds.

Figure 8 shows the expanded mass scale spectra of M6 subfraction at $m/z$ 570, 584, and 586, which were internally

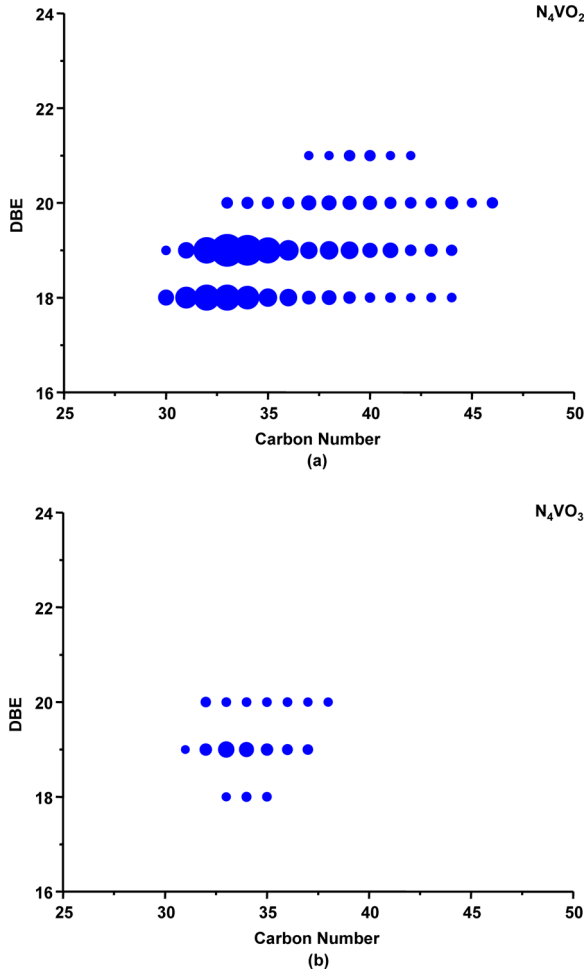


**Figure 10.** Iso-abundant plots of DBE as a function of the carbon number: (a and b) for $N_4VO_2$ and $N_4VO_3$ in subfraction M5 derived from positive-ion ESI FT-ICR MS, respectively.

calibrated with $[C_{41}H_{63}N_1 + H]^+$, $[C_{42}H_{65}N_1 + H]^+$, and $[C_{42}H_{67}N_1 + H]^+$, respectively. Initially, $C_nH_mN_4V_1O_2$, $C_nH_mN_4V_1O_3$, and $C_nH_mN_4V_1O_4$ compounds were detected in the crude oil sample by FT-ICR MS analysis. Identification of these porphyrin compounds was performed by assigning the spectrum peaks to accurate mass values and isotopic masses and observing their characteristic serial distribution at the large mass range. These vanadium compounds had DBE values of 18, 19, and 20, which are similar to vanadyl porphyrins. Figure 9 shows the iso-abundance plots of DBE as a function of the carbon number for these three $N_4VO_n$ class vanadium compounds in the M6 subfraction. The $C_nH_mN_4V_1O_2$ and $C_nH_mN_4V_1O_3$ class species exhibited five types of compounds, with DBE values of 18, 19, 20, 21, and 22. In contrast, the $C_nH_mN_4V_1O_4$ class species exhibited three types of compounds, with DBE values of 19, 20, and 21. The most abundant $C_nH_mN_4V_1O_2$ and $C_nH_mN_4V_1O_3$ class species in the M6 subfraction had DBE values of 18 and 19, whereas the $C_nH_mN_4V_1O_4$ class species had DBE = 19. The range of carbon numbers for these vanadium compounds was $C_{28}$–$C_{45}$, with the center of mass at $C_{32}$.

The three vanadium compounds with additional oxygen atoms were not found in the M4 subfraction. However, $C_nH_mN_4V_1O_2$ and $C_nH_mN_4V_1O_3$ class species were detected in the M5 subfraction. Figure 10 shows the iso-abundance plots of


dx.doi.org/10.1021/ef400161p | Energy Fuels 2013, 27, 2874–2882

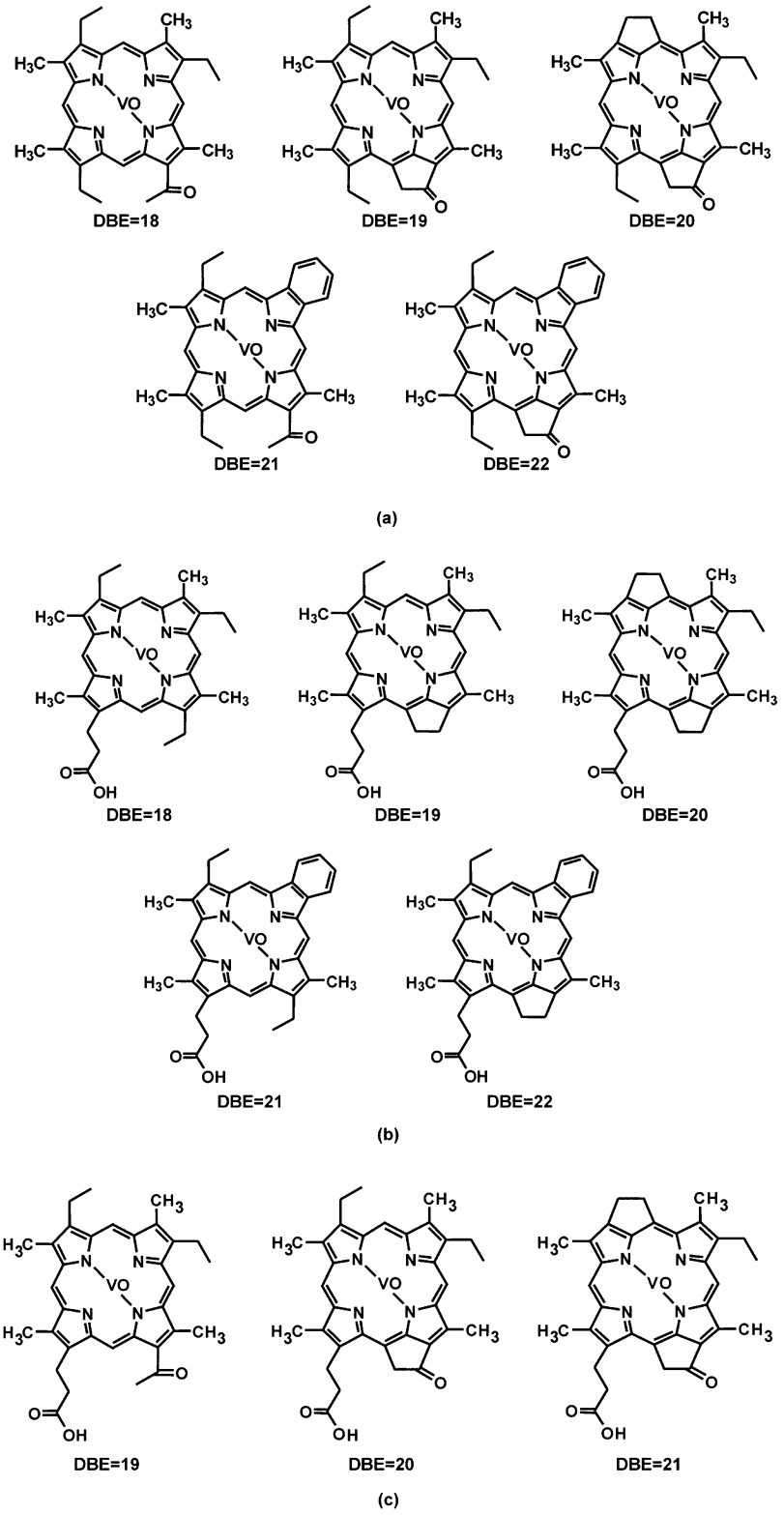


**Figure 11.** Proposed structures of new class species of vanadium compounds in Venezuela Orinoco crude oil subfractions M5 and M6: (a) for $N_4V_1O_2$, (b) for $N_4V_1O_3$, and (c) for $N_4V_1O_4$. DBE is the number of rings plus double bonds to carbon.

DBE as a function of the carbon number for $C_nH_mN_4V_1O_2$ and $C_nH_mN_4V_1O_3$ class species in the M5 subfraction. The $C_nH_mN_4V_1O_2$ and $C_nH_mN_4V_1O_3$ class species exhibited four and three types of compounds, respectively, with DBE values of 18, 19, 20, and 21. Because M4, M5, and M6 were obtained by sequential elution with solvents of increased polarity, the vanadium compounds with more oxygen atoms and/or high DBE values were enriched in the high-polarity subfractions.

Figure 11 shows the possible structures of the three newly identified vanadium compounds based on the Treibs theoretical model on the formation of porphyrins from the evolution of chlorophyll and hemes.[2,3] These molecular structures had


dx.doi.org/10.1021/ef400161p | *Energy Fuels* 2013, 27, 2874−2882

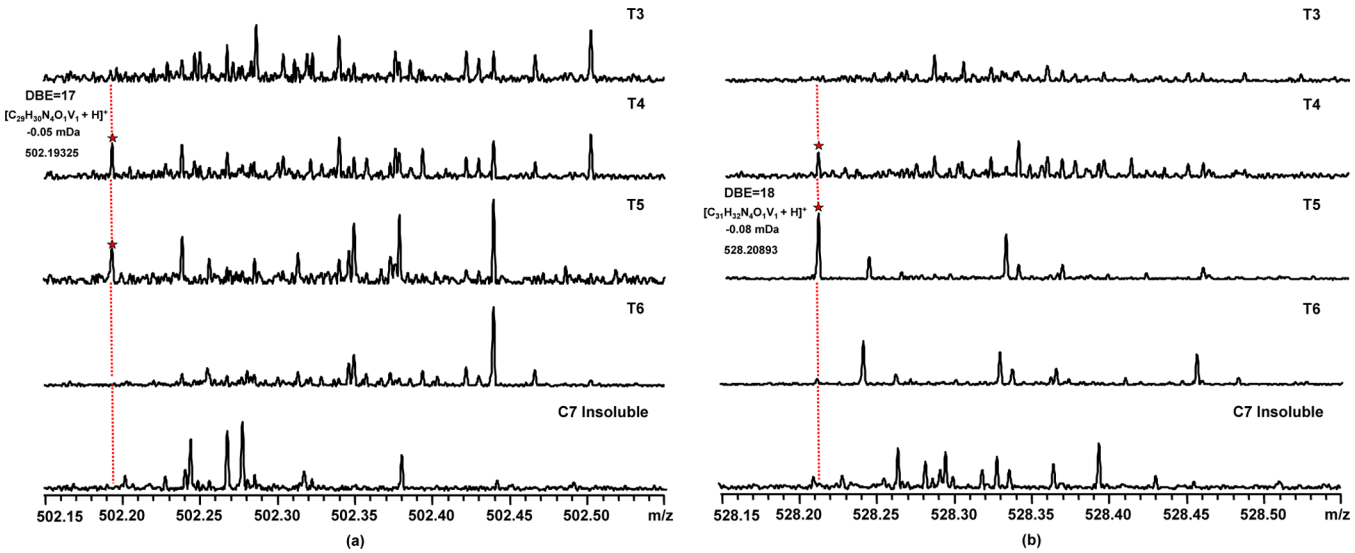


**Figure 12.** Expanded mass scale spectra of subfractions T3, T4, T5, and T6 and $nC_7$ insolubles of toluene extraction from the positive-ion ESI FT-ICR MS analysis: (a and b) at $m/z$ 502 and 528, respectively.

varying DBE values and oxygen atoms, with functional groups of carbonyl and/or carboxyl at the peripheral of the porphyrin structure.

Identification of $C_nH_mN_4V_1O_2$, $C_nH_mN_4V_1O_3$, and $C_nH_mN_4V_1O_4$ class species in crude oil is significant to the petroleum geochemistry and supports the hypothesis that petroporphyrins were derived from chlorophylls and hemes.

**3.5. Characterization of Vanadyl Porphyrins in Toluene-Extracted Fractions by Positive-Ion ESI FT-ICR MS.** Among the toluene-extracted fractions, the most abundant vanadium compounds were found in $nC_7$ insolubles, T3, T4, and T5 subfractions, as shown in Table 1. Figure 12 shows the expanded mass scale spectra of T3, T4, T5, and T6 subfractions and $nC_7$ insolubles at $m/z$ 502 and 528. The ETIO and DPEP were found in the T4 and T5 subfractions. It is not possible to have complete extraction of all vanadyl porphyrins in a petroleum sample. As discussed, T4 and T5 subfractions exhibited characteristic UV−vis absorption bands of vanadyl porphyrins. These porphyrins likely exhibit similar structures to those in the methanol extracts. The iso-abundance plots of DBE as a function of the carbon number for vanadyl porphyrins in T4 and T5 subfractions derived from positive-ion ESI FT-ICR mass spectra are shown in panels a and b of Figure S2 of the Supporting Information. Most of the ETIO and DPEP with long side chains were eluted in the T4 subfraction. The porphyrins in the T5 subfraction were mostly $C_{28}$−$C_{33}$ DPEP, with a center of mass at $C_{31}$.

However, no vanadium species in the T3 subfraction and $nC_7$ insolubles was detected by ESI FT-ICR MS, although a high vanadium concentration was detected and the UV−vis spectra of T3 showed the characteristic absorption peak for vanadyl porphyrin. There may be an explanation: some vanadium compounds with the porphyrin macrocycle existed in T3, which may contain some other heteroatoms, and some unknown vanadium compounds were concentrated in $nC_7$ insolubles.

It should be noted that the vanadium compounds in the T3 subfraction and $nC_7$ insolubles accounted for 22.66% of the total vanadium in the feedstock. However, the molecular structures of these vanadium compounds were not identified. Further purification and the application of the hyphenated technique between HPLC and inductively coupled plasma−mass spectrometry (ICP−MS) may potentially reveal the identity of these compounds. FT-ICR MS would be the most effective way to identify these vanadium compounds in a complex matrix, such as heavy crude oil.

## 4. CONCLUSION

Detailed characterization of vanadyl porphyrins was performed on Venezuela Orinoco heavy crude oil by ESI FT-ICR MS. All six types of petroleum vanadyl porphyrins were detected. Three new series of vanadyl porphyrins corresponding to molecules of $C_nH_mN_4VO_2$, $C_nH_mN_4VO_3$, and $C_nH_mN_4VO_4$ were identified by ESI FT-ICR MS. In addition, non-porphyrins were concentrated in some subfractions, and these compounds accounted for 22.66% of total vanadium in the feedstock; however, the molecular structures of these compounds were not determined in this study.

## ■ ASSOCIATED CONTENT

### Ⓢ Supporting Information

Iso-abundant plots of DBE as a function of the carbon number for each type of vanadyl porphyrins in Venezuela crude oil (Figure S1) and subfractions T4 and T5 (panels a and b of Figure S2) derived from positive-ion ESI FT-ICR MS. This material is available free of charge via the Internet at http://pubs.acs.org.

## ■ AUTHOR INFORMATION

### Corresponding Author

*Telephone: +86-10-8973-3392 (C.X.); +86-10-8973-3738 (Q.S.). E-mail: xcm@cup.edu.cn (C.X.); sq@cup.edu.cn (Q.S.).

### Notes

The authors declare no competing financial interest.

## ■ ACKNOWLEDGMENTS

This work was supported by the National Natural Science Foundation of China (NSFC, 21236009) and the National Basic Research Program of China (2010CB226901).

## REFERENCES


(1) Dechaine, G. P.; Gray, M. R. *Energy Fuels* **2010**, *24* (5), 2795−2808.
(2) Treibs, A. *Ann. Chem.* **1934**, *510*, 42−62.
(3) Treibs, A. *Angew. Chem.* **1936**, *49*, 682−686.
(4) McKenna, A. M.; Purcell, J. M.; Rodgers, R. P.; Marshall, A. G. *Energy Fuels* **2009**, *23* (4), 2122−2128.
(5) Wang, X.; Lang, R.; Qi, L. *Geochemistry* **1983**, *2* (3), 251−260.
(6) Liao, Z.; Huang, D. *Sci. China, Ser. B: Chem.* **1990**, *33* (5), 631−640.
(7) Márquez, N.; Ysambertt, F.; De La Cruz, C. *Anal. Chim. Acta* **1999**, *395* (3), 343−349.
(8) Xu, H.; Yu, D.; Que, G. *Fuel* **2005**, *84* (6), 647−652.
(9) Xu, H.; Que, G.; Yu, D. *Energy Fuels* **2005**, *19* (2), 517−524.
(10) Eskins, K.; Scholfield, C. R.; Dutton, H. J. *J. Chromatogr., A* **1977**, *135* (1), 217−220.
(11) Quirke, J. M. E.; Eglinton, G.; Maxwell, J. R. *J. Am. Chem. Soc.* **1979**, *101* (26), 7693−7697.
(12) Quirke, J. M. E.; Shaw, G. J.; Soper, P. D.; Maxwell, J. R. *Tetrahydron* **1980**, *36* (22), 3261−3267.
(13) Quirke, J. M. E.; Eglinton, G.; Palmer, S. E.; Baker, E. W. *Chem. Geol.* **1982**, *35* (1−2), 69−85.
(14) Mozzhelina, T. K.; Serebrennikova, O. V.; Beiko, O. A.; Krasovskaya, L. I. *Pet. Chem. U.S.S.R.* **1985**, *25* (3), 189−196.
(15) Fish, R. H.; Komlenic, J. J. *Anal. Chem.* **1984**, *56* (3), 510−517.
(16) Senko, M. W.; Hendrickson, C. L.; Pasa-Toli, L.; Marto, J. A.; White, F. M.; Guan, S.; Marshall, A. G. *Rapid Commun. Mass Spectrom.* **1996**, *10* (14), 1824−1828.
(17) Marshall, A. G.; Rodgers, R. P. *Acc. Chem. Res.* **2003**, *37* (1), 53−59.
(18) Rodgers, R. P.; Marshall, A. G. *Petroleomics: Advanced Characterization of Petroleum-Derived Materials by Fourier Transform Ion Cyclotron Resonance Mass Spectrometry (FT-ICR MS)*; Springer: New York, 2005; pp 63−93.
(19) Rodgers, R. P.; Schaub, T. M.; Marshall, A. G. *Anal. Chem.* **2005**, *77* (1), 20A−27A.
(20) Marshall, A. G.; Rodgers, R. P. *Proc. Natl. Acad. Sci. U.S.A.* **2008**, *105* (47), 18090−18095.
(21) McLafferty, F. W. *Proc. Natl. Acad. Sci. U.S.A.* **2008**, *105* (47), 18088−18089.
(22) Rodgers, R. P.; Hendrickson, C. L.; Emmett, M. R.; Marshall, A. G.; Greaney, M.; Qian, K. *Can. J. Chem.* **2001**, *79* (5−6), 546−551.
(23) Qian, K.; Mennito, A. S.; Edwards, K. E.; Ferrughelli, D. T. *Rapid Commun. Mass Spectrom.* **2008**, *22* (14), 2153−2160.
(24) Qian, K.; Edwards, K. E.; Mennito, A. S.; Walters, C. C. *Anal. Chem.* **2010**, *82* (1), 413−419.
(25) Chen, X.; Sun, Y.; Yu, X.; Yang, C. *Spec. Petrochem.* **2002**, *2*, 57−58.
(26) Shi, Q.; Pan, N.; Long, H.; Cui, D.; Guo, X.; Long, Y.; Chung, K. H.; Zhao, S.; Xu, C.; Hsu, C. S. *Energy Fuels* **2013**, *27* (1), 108−117.
(27) Freeman, D. H.; Saint Martin, D. C.; Boreham, C. J. *Energy Fuels* **1993**, *7* (2), 194−199.
(28) Yen, T. F. Chemical aspects of metals in native petroleum. In *The Role of Trace Metals in Petroleum*; Yen, T. F., Ed.; Ann Arbor Science Publishers, Inc.: Ann Arbor, MI, 1975; pp 1−30.